Confinement-Induced Solidification of Colloid-Polymer Depletion Mixtures

Melissa Spannuth[1,*] and Jacinta C. Conrad[1,2,†]

[1]Department of Chemical and Biomolecular Engineering, University of Houston, Houston, Texas 77204, USA
[2]Petroleum Engineering Program, University of Houston, Houston, Texas 77204, USA

(Received 9 December 2011; published 9 July 2012)

Using a model colloid-polymer suspension, we show that confinement induces solidification in attractive colloidal suspensions via a fundamentally different route from that active in hard sphere colloidal suspensions. For a range of polymer concentrations, the suspensions undergo a phase transition from a colloidal fluid of clusters to a colloidal gel as confinement increases while polymer and particle concentration are held constant. In both fluid- and solidlike attractive suspensions, effects of confinement on the structure and dynamics appear at much larger thicknesses than for hard-sphere suspensions. The solidification does not originate from structuring of the colloids by the walls. Instead, by analyzing cluster size distributions in the fluid phase and particle dynamics in the gel phase as a function of confinement, we find that the strength of the effective interparticle attraction increases as the samples are confined. We show that the increase in the effective attraction can be understood as a consequence of the increasing importance of excluded volume due to the walls to the free energy of the polymer as confinement is increased.

DOI: 10.1103/PhysRevLett.109.028301 PACS numbers: 82.70.Dd, 47.57.J−, 64.75.Xc

Confining a material profoundly affects its phase behavior as well as its structural and mechanical properties (see, e.g., [1] and references therein), but the effects of confinement can be difficult to study in atomic or molecular systems due to the small length scales and short time scales involved. Colloidal suspensions are an ideal system in which to investigate effects of confinement, as particles with controlled interparticle interactions can be directly visualized. For colloids interacting via a hard-sphere or charged-sphere potential, confinement induces the formation of two types of colloidal solids, equilibrium crystals [2] and nonequilibrium glasses [3], at particle volume fractions ϕ below those required in bulk. Wall-induced structuring of particles plays a critical role in these solidification transitions. The formation of layers of oscillating density at container walls leads to crystallization in confinement [4,5]. Similarly, the enhancement of glassy structural order near walls leads to slowed particle dynamics and early vitrification [3,6]. Both types of phase transition require confinement to a length scale of about 10–20 times the particle size.

Suspensions in which the particles experience an attractive interaction can undergo phase separation that leads to new colloidal phases such as fluids of clusters and gels. The effect of confinement on this phase separation is not understood. Numerical simulations predict that confinement should alter the onset and dynamics of phase separation due to the greater affinity of one phase for the walls [7,8]. Indeed, capillary condensation of a colloidal liquid from a colloidal gas is observed in confined colloid-polymer mixtures [9]. For soft microgel particles, spinodal phase separation leads to gelation in confinement, but ϕ increases simultaneously with confinement in this system, which may have itself caused the gelation [10].

In this Letter we study a colloid-polymer mixture in which the strength and range of the effective attraction can be precisely tuned at constant ϕ and the confinement independently controlled. We find that confinement induces solidification in colloid-polymer depletion mixtures via a physical mechanism that is fundamentally different from that active in hard-sphere suspensions: a change in the strength of the effective interparticle attraction, deduced from broadening of the distribution of cluster sizes in fluids of clusters and a decrease in the probability of large particle displacements in gels. Surprisingly, the effect is already evident at very large thicknesses of up to 70 times the particle diameter. We hypothesize that the apparent increase in effective attraction arises from the increasing contribution of the walls to the total excluded volume as confinement increases, which affects the free energy of the polymers.

Our model system consists of $2a = 0.865$ μm diameter poly(methyl methacrylate) particles (polydispersity $\approx$ 15%) sterically stabilized with poly(12-hydroxystearic acid) and dispersed in a 3:1 mixture of decahydronaphthalene (DHN) and cyclohexylbromide (CXB) to match the density and index of refraction of the particles. To minimize effects of gravity, we add CXB or DHN dropwise and confirm that clusters remain in suspension after centrifugation at 800 g for 1.25 h. In these solvents the particles are charged [11], so we add tetrabutylammonium chloride salt to a concentration of 1.5 mM to partially screen the charges [12]. To induce an effective depletion attraction between particles, we use polystyrene (molecular weight $M_w =$ 295.8 kDa) with a radius of gyration $R_g = 15$ nm [13] and an overlap concentration $C_p^* = 3M_w/4\pi R_g^3 N_A \approx$ 35 mg/mL. We fix the particle volume fraction $\phi \approx 0.15$ and vary the polymer concentration C_p between 0 and 23.6 mg/mL (Table I). Increasing C_p increases the

TABLE I. Volume fraction and polymer concentration of samples.

Sample	1	2	3	4	5	6	7
ϕ	0.147	0.148	0.147	0.153	0.149	0.148	0.151
C_p [mg/mL]	0.0	10.4	12.9	15.5	17.7	20.7	23.6

strength of attraction between the particles while maintaining a constant range of attraction $\xi = R_g/a \approx 0.035$.

Samples flow by capillary suction into wedge-shaped glass chambers with nearly parallel walls (opening angle $<0.5°$). Bulk rheology indicates that at the shear rates applied during loading, our samples behave as either Newtonian or shear-thinning fluids, suggesting that samples are fully homogenized. After filling, samples sit undisturbed for 30 minutes before observation by confocal fluorescence microscopy (Visitech VT-Infinity). We acquire three-dimensional image stacks at various positions along the wedge corresponding to different thicknesses h. We then use standard algorithms [14] to locate all particles in three dimensions and track their motion in two dimensions at the midplane of the chamber ($z = h/2$).

Confocal micrographs show that samples become increasingly solidlike with either increasing C_p at constant h or increasing confinement at constant C_p (e.g., Fig. 1, center left column). We identify four different colloidal phases among the samples. Colloidal crystals are determined directly from confocal images and by their unique particle pair correlation function $g(r)$. Colloidal fluids are characterized by the absence of long-range order and the presence of a fluid peak in $g(r)$ (Fig. 1, bottom row, center columns), whereas $g(r)$ for fluids of clusters exhibits a distinct cluster peak and clusters are visible in confocal images (Fig. 1, middle row, center columns). We define the colloidal gel via connectivity percolation: a gel contains a spanning cluster in three dimensions (Fig. 1, top row, center columns). We obtain similar results using a dynamical metric based on the magnitude and slope of the mean squared displacement (MSD, Fig. 1, right column) [15].

The resulting phase diagram shown in Fig. 1 demonstrates how confinement-induced solidification changes with the strength of the interparticle attraction. At low C_p, samples crystallize when confined below about $16a - 35a$, as observed previously (e.g., [2,16]). At high C_p, samples form a gel at all h as expected [17,18]. Interestingly, at intermediate C_p, samples transform from fluids of clusters to gels ($C_p = 15.5$ and 17.7 mg/mL) and in one case ($C_p = 12.9$ mg/mL) from a crystal to a gel. We have independently confirmed that both ϕ and C_p remain constant over the range of h observed, by respectively measuring particle density via Voronoi volumes and solvent viscosity via particle-tracking microrheology. Our measurement is therefore the first observation of confinement-induced gelation at constant ϕ and C_p. In the remainder of this Letter, we show that this solidification arises from a new and unanticipated physical mechanism.

In confined systems wall-induced structuring plays an integral role in the phase behavior. In hard-sphere systems, structural changes induced by walls drive solidification of colloidal fluids into crystals, via layering [4,5], or glasses, via glassy structural order [3,6]. Wall-induced layering also appears in phase-separating colloid-polymer mixtures that do not solidify [7]. We therefore look for wall-induced layering in confined attractive suspensions. In fluid samples at low C_p, we indeed observe strong wall layering (Fig. 2, left) that leads to crystallization in confinement. However, the number of layers decreases as more or larger clusters form in the fluids (Fig. 2, center). Layers are not present in gels (Fig. 2, right), even at large h and high C_p. Several other structural measures, such as the average

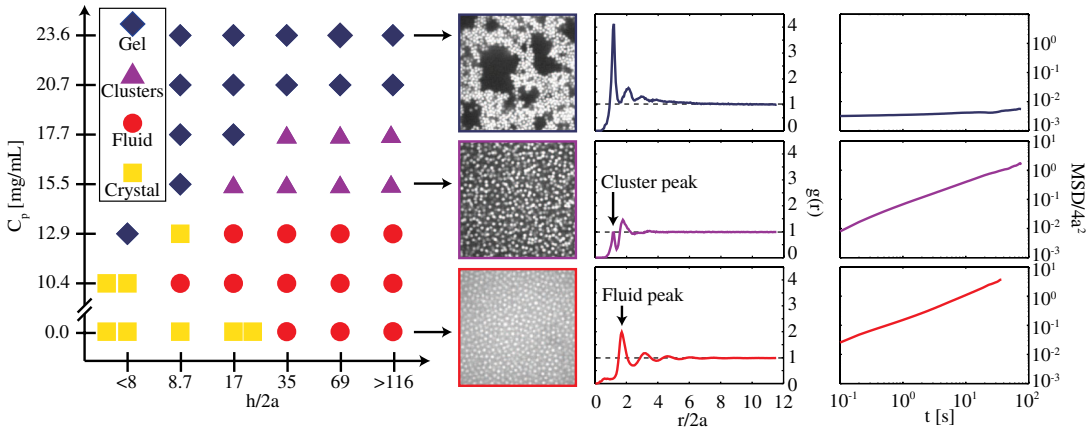

FIG. 1 (color online). Polymer concentration versus confinement phase diagram (left) derived from confocal images (center left), particle pair correlation functions (center right), and mean squared displacements (MSD, right). Shapes and colors indicate the phase: crystal (yellow squares), fluid (red circles), fluid of clusters (purple triangles), and gel (blue diamonds). From top to bottom, the images and correlation functions show representative examples of a gel (sample 7 at $h/2a = 8.7$), a fluid of clusters (sample 4 at $h/2a = 17$), and a colloidal fluid (sample 1 at $h/2a > 116$).

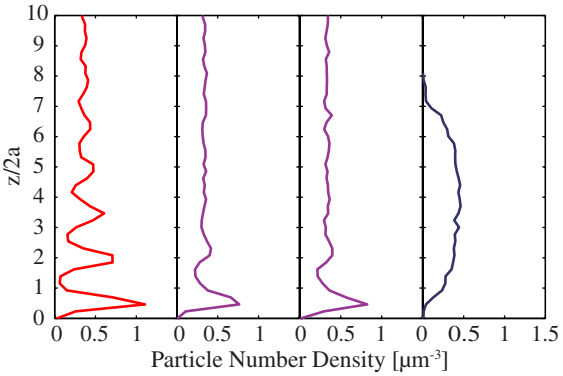

FIG. 2 (color online). Typical particle number density profiles for the different phases: from left to right, fluid (sample 1 at $h/2a > 116$), fluids of clusters (sample 4 at $h/2a = 35$ and 17), and gel (sample 4 at $h/2a = 8.7$). Only the region near the lower chamber wall is shown. The location of the first nonzero density is taken as $z/2a = 0$, which is approximately 0.43 μm from the chamber wall because particles are located by their centers. Colors indicate the phase as in Fig. 1.

number of bonds per particle, the fraction of particles in clusters, the average cluster size, and the cluster number density do not show any significant variation across the chamber thickness, except in the gel phase where most measures increase towards the chamber midplane. Thus, in our system wall-induced layering is not responsible for solidification. Instead, by examining the cluster size distributions, we show that confinement increases the effective attraction between particles.

The connection between the size distribution of clusters in a colloidal fluid and the strength of attraction between particles was demonstrated by Lu *et al.* [18]. They showed that in colloidal fluids approaching gelation at constant ϕ the cluster size distribution $n(s)$ was determined solely by the reduced second virial coefficient $B_2^* = (3/8a^3)\int_0^\infty [1 - \exp(-U(r)/k_BT)]r^2dr$, where $U(r)$ is the particle pair potential and k_BT is the thermal energy [19]. Regardless of the form chosen for $U(r)$, $n(s)$ maintained the same shape as long as B_2^* was the same. Because $n(s)$ corresponds one-to-one with B_2^* and B_2^* is an integral of $U(r)$ for short-ranged potentials, changes in $n(s)$ reflect changes in $U(r)$. Indeed, Lu *et al.* [18] found that the broadening of $n(s)$ with increasing C_p that they observed experimentally could be mapped uniquely to increasing values of B_2^*, from which U/k_BT could then be calculated (e.g., using the Asakura-Oosawa potential for the depletion interaction in colloid-polymer mixtures [20]).

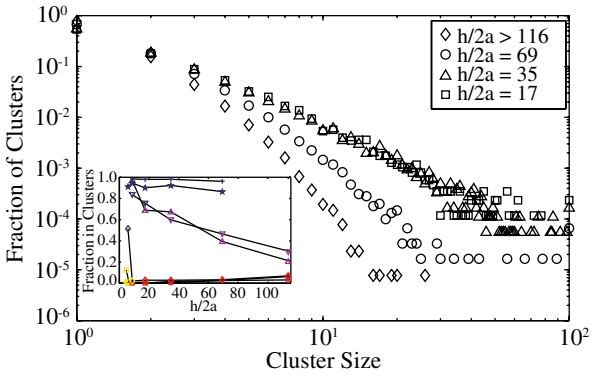

FIG. 3 (color online). Cluster size distributions in a fluid of clusters (sample 4) as a function of confinement. Inset: fraction of particles participating in clusters for samples 1(○), 2(□), 3(◇), 4(△), 5(▽), 6(☆), and 7(+). Colors indicate the phase as in Fig. 1.

To investigate the influence of confinement on interparticle interactions, we therefore examine $n(s)$ (Fig. 3). In fluids of clusters (samples 4 and 5), the cluster size distribution broadens with increasing confinement at constant C_p and tends towards a power law near gelation. According to the results of Lu *et al.* [18], these changes in $n(s)$ imply that the strength of attraction between particles increases in confinement. This increase is further supported by changes in $g(r)$, which is related to $U(r)$. With increasing confinement the heights of the cluster and fluid peaks increase and decrease respectively (Fig. 4), consistent with the changes seen for increasing strength of attraction. Simultaneously with the broadening of $n(s)$, the fraction of particles participating in clusters of any size increases (Fig. 3 inset). At gelation, nearly all particles are trapped in clusters. This gradual increase in cluster participation is also consistent with an increase in the strength of the effective attraction between particles.

Unexpectedly, the change in the interaction is strong enough for the system to experience its effects for even

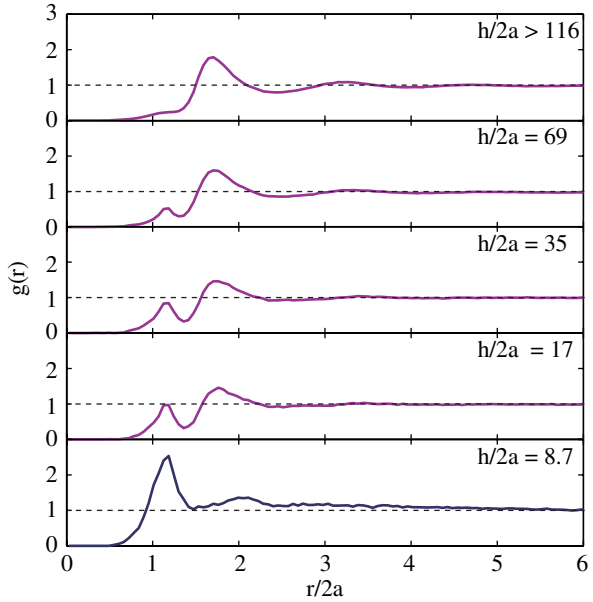

FIG. 4 (color online). Pair correlation functions in sample 4 at $h/2a > 116$ and $h/2a = 69$, 35, 17, and 8.7 from top to bottom. Sample is a fluid of clusters at all h except $h/2a = 8.7$, which is a gel. Colors indicate the phase as in Fig. 1.

modest confinement ($h/2a = 69$). Typically, hard-sphere suspensions must be confined to $h/2a \approx 10$–20 before wall effects are felt throughout the material, whereas here we see confinement effects at $h/2a \approx 70$. This observation further highlights that the mechanism for confinement-induced solidification in attractive suspensions is not simply driven by layering of the colloids at the walls, but by a much longer-ranged mechanism.

We also find evidence of increasing effective attraction strength in samples that are gels at all h (samples 6 and 7). For gels, $n(s)$ does not vary with h, so we instead examine the particle dynamics. For the weaker gel in sample 6, the particle MSD slows and becomes more subdiffusive with decreasing h, similar to what we observe for fluids with clusters in samples 4 and 5 [Fig. 5(a) inset]. For the stronger gel in sample 7, the MSD appears arrested for all h [Fig. 5(b) inset], but we can still discern differences in dynamics through the self-part of the van Hove correlation function $G_s(x, \tau) = (1/N)\Sigma_{i=1}^{N} \delta[x + x_i(0) - x_i(\tau)]$ [21]. This represents the probability of a displacement x occurring over a time τ. We calculate $G_s(x, \tau)$ at the chamber midplane (i.e., $z = h/2$) for $\tau = 10$ s, which is approximately 10 times longer than the self-diffusion time of a free particle. In fluids both with and without clusters, $G_s(x, \tau)$ has a Gaussian shape reflecting diffusion of free particles and clusters [Fig. 5(a)]. In gels, $G_s(x, \tau)$ acquires a sharp Gaussian peak around $x = 0$ and broad exponential tails [Fig. 5(b)] reflecting two distinct types of particle dynamics: caged motion and sporadic large hops [22,23]. As gels are confined, the exponential tails steepen indicating that large displacements become less probable [Fig. 5(b)], consistent with the increasingly arrested dynamics expected for stronger attraction [15,17]. Thus, even in samples that are gels in bulk, confinement alters the effective interparticle interactions and hence the material properties.

The results presented here demonstrate that confinement increases the strength of the effective interparticle attraction. We hypothesize that this increase results from changes in the volume available to the polymer in confinement. In colloid-polymer mixtures, the effective interparticle attraction arises from the decrease in free energy produced by the increase in volume available to the polymers when the excluded volumes around particles overlap. The free energy due to the polymers can be written as $F = F_{\mathrm{id}} - Nk_BT \ln(V_A/V)$, where F_{id} is the contribution to the free energy treating the polymers as an ideal gas, N is the number of polymers, V_A is the volume accessible to the polymers, and V is the total volume. In a confined colloid-polymer system, $V_A = V - V_p + V_o - V_w$, where V_p is the particle excluded volume, V_o the overlap volume, and V_w the additional excluded volume at the chamber walls that by analogy to V_p is proportional to R_g. As confinement increases at constant ϕ and C_p, V_w/V increases while V_p/V remains constant; the only way to maximize V_A/V and hence minimize the free energy is to increase the overlap volume V_o/V. Thus, even modest confinement increases the number of particles in close contact, thereby increasing the effective attraction among the particles and resulting in the growth of clusters and eventually gelation. This argument suggests via Taylor series expansion of $\ln(V_A/V)$ that the C_p required for gelation scales as $1/h$, which is in qualitative agreement with our data. This effect is particularly long-ranged because the free energy depends logarithmically on the ratio V_A/V, so even small changes to this ratio (e.g., at $h/2a = 69$, $V_w/V \sim R_g/69a \approx 5 \times 10^{-4}$) can produce large changes in the free energy and effective attraction. The height at which we detect changes depends on the sensitivity of our cluster size measurement; techniques that can measure smaller changes in the interparticle potential may observe confinement-induced attractions at even larger thicknesses.

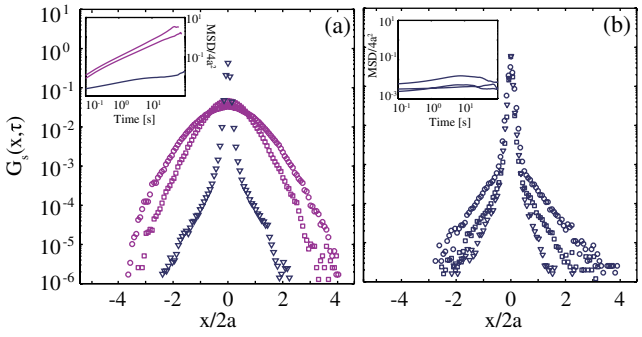

FIG. 5 (color online). Self-part of the van Hove correlation function and (inset) mean squared displacement for samples 4 (a) and 7 (b) as a function of confinement ($h/2a = 69$ [○], 17 [□], and 8.7 [▽]). In (a), the sample is a fluid of clusters for $h/2a = 69$ and 17, but a gel for $h/2a = 8.7$. In (b), the sample is a gel for all h.

Particle aggregation is not the only route to increase the available volume and decrease the free energy. In our open system, where confined regions are connected to bulk regions, particles and polymers can migrate along the chamber and lower the free energy contributed by highly confined regions. Over long times this may lead to disintegration of the clusters and gels; indeed, preliminary experiments on the long-time evolution of our samples indicate that particle migration may occur in some cases. Determining when and to what extent this will occur requires considering the contribution of the particles to the total free energy of the system.

The confinement-induced structural and dynamic changes in model attractive suspensions demonstrated here are important to applications requiring attractive colloidal suspensions to be spread into thin films [24] or flow through constrained geometries [25] and suggest novel routes for controlling structure formation in colloidal materials. Similar effects might be seen in other types of gels when confined, e.g., the networks of actin present in the lamellipodia that enable cell motion [26]. We expect the proposed physical mechanism to apply in any system

where the free energy and interactions are governed by available volume, such as polymer blends or brush-coated nanoparticles. Finally, these results raise new questions for further study, such as the validity of the A-O potential for confined systems and the ingredients for a microscopic theory, how to measure the excluded volume at the wall, and the applicability of analogies to 2D systems in which effective surface concentration is reduced while number concentration is held constant.

We acknowledge the Texas Center for Superconductivity and the UH GEAR program for seed funding. We thank M. Doxastakis, R. Krishnamoorti, S. Kumar, and A. Mohraz for helpful comments.

*melissa.spannuth@gmail.com
†jcconrad@uh.edu

[1] J. E. Hug, F. van Swol, and C. F. Zukoski, Langmuir **11**, 111 (1995).
[2] P. Pieranski, L. Strzelecki, and B. Pansu, Phys. Rev. Lett. **50**, 900 (1983).
[3] C. R. Nugent, K. V. Edmond, H. N. Patel, and E. R. Weeks, Phys. Rev. Lett. **99**, 025702 (2007).
[4] D. H. Van Winkle and C. A. Murray, J. Chem. Phys. **89**, 3885 (1988).
[5] A. Fortini and M. Dijkstra, J. Phys. Condens. Matter **18**, L371 (2006).
[6] K. Watanabe, T. Kawasaki, and H. Tanaka, Nature Mater. **10**, 512 (2011).
[7] K. Binder, J. Horbach, R. Vink, and A. De Virgiliis, Soft Matter **4**, 1555 (2008).
[8] K. Binder, S. Puri, S. K. Das, and J. Horbach, J. Stat. Phys. **138**, 51 (2010).
[9] D. G. A. L. Aarts and H. N. W. Lekkerkerker, J. Phys. Condens. Matter **16**, S4231 (2004).
[10] P. S. Sarangapani, Y. Yu, J. Zhao, and Y. Zhu, Phys. Rev. E **77**, 061406 (2008).
[11] A. Yethiraj and A. van Blaaderen, Nature (London) **421**, 513 (2003).
[12] Samples prepared with higher concentrations of salt exhibit the same behavior as reported here.
[13] G. C. Berry, J. Chem. Phys. **44**, 4550 (1966).
[14] J. C. Crocker and D. G. Grier, J. Colloid Interface Sci. **179**, 298 (1996).
[15] M. H. Lee and E. M. Furst, Phys. Rev. E **77**, 041408 (2008).
[16] D. H. Van Winkle and C. A. Murray, Phys. Rev. A **34**, 562 (1986).
[17] C. J. Dibble, M. Kogan, and M. J. Solomon, Phys. Rev. E **74**, 041403 (2006).
[18] P. J. Lu, E. Zaccarelli, F. Ciulla, A. B. Schofield, F. Sciortino, and D. A. Weitz, Nature (London) **453**, 499 (2008).
[19] M. G. Noro and D. Frenkel, J. Chem. Phys. **113**, 2941 (2000).
[20] S. Asakura and F. Oosawa, J. Chem. Phys. **22**, 1255 (1954).
[21] A. Rahman, Phys. Rev. **136**, A405 (1964).
[22] Y. Gao and M. L. Kilfoil, Phys. Rev. Lett. **99**, 078301 (2007).
[23] Y. Gao and M. L. Kilfoil, Phys. Rev. E **79**, 051406 (2009).
[24] L. T. Shereda, R. G. Larson, and M. J. Solomon, Phys. Rev. Lett. **101**, 038301 (2008).
[25] J. E. Smay, J. Cesarano III, and J. A. Lewis, Langmuir **18**, 5429 (2002).
[26] J. Stricker, T. Falzone, and M. L. Gardel, J. Biomech. **43**, 9 (2010).